QSAR-guided semi-synthesis and in vitro validation of antiplasmodial activity in ursolic acid derivatives

ARTICLE *in* RSC ADVANCES · MARCH 2015

Impact Factor: 3.84 · DOI: 10.1039/c4ra13709d

6 AUTHORS, INCLUDING:

Harveer Cheema
Central Institute of Medicinal and Aromatic …
7 PUBLICATIONS **14** CITATIONS
SEE PROFILE

Himanshu Tripathi
Central Institute of Medicinal and Aromatic …
6 PUBLICATIONS **7** CITATIONS
SEE PROFILE

Feroz Khan
CSIR-Central Institute of Medicinal and Aro…
131 PUBLICATIONS **528** CITATIONS
SEE PROFILE

Santosh Srivastava
Central Institute of Medicinal and Aromatic …
136 PUBLICATIONS **1,059** CITATIONS
SEE PROFILE

RSC Advances

PAPER

Cite this: *RSC Adv.*, 2015, **5**, 32133

QSAR-guided semi-synthesis and *in vitro* validation of antiplasmodial activity in ursolic acid derivatives†

Komal Kalani,‡§[ad] Harveer Singh Cheema,§[bd] Himanshu Tripathi,[cd] Feroz Khan,[cd] M. P. Daroker[bd] and Santosh Kumar Srivastava*[ad]

As a part of our antimalarial drug discovery programme, a quantitative structure–activity relationship (QSAR) model was developed for the prediction of antiplasmodial activity in ursolic acid (UA) derivatives, followed by the wet laboratory semi-synthesis of virtually active derivatives and their *in vitro* biological evaluation. The QSAR model was developed by a forward stepwise multiple linear regression method using a leave-one-out approach, which showed a 96% prediction accuracy. The most active virtual derivatives of UA were semi-synthesized and their *in vitro* evaluation showed a similar antiplasmodial activity to the predicted one, thus validating the QSAR model. Further, the *in silico* mode of action was studied on β-hematin and subsequently confirmed by *in vitro* FPIX biomineralization inhibition activity. Finally, the *in silico* ADME/T properties and cytotoxicity against Vero cells using an MTT assay were studied. Out of eight derivatives, the two UA-18 and UA-21 showed significant dose-dependent antiplasmodial activity in arresting the progress of *P. falciparum* erythrocytic cycle. Furthermore, the *in silico* and *in vitro* mode of action studies of these derivatives showed comparable binding energies and percentage inhibitions on β-hematin to that of the standard drug chloroquine (CQ). The *in silico* ADME/T analysis of UA and its derivatives did not show CYP2D6 inhibition, hepatotoxicity nor mutagenicity, but showed a poor solubility and poor human intestinal absorption. These findings may be of immense importance in antiplasmodial drug development from an inexpensive and widely available natural product, *i.e.* ursolic acid.

Received 3rd November 2014
Accepted 18th March 2015

DOI: 10.1039/c4ra13709d

www.rsc.org/advances

1. Introduction

For centuries, malaria has undoubtedly been the single most destructive disease in developing countries.[1] According to WHO, this disease has placed about 3.3 billion people in danger and has become an enormous global health challenge. Although recommended preventive drugs, such as a combination of sulfadoxine, pyramethamine and amodiaquine are available,[2] the burden of this disease is getting worse, mainly due to the increasing resistance of *Plasmodium falciparum* against the widely available anti-malarial drugs.[3] Known natural molecules such as artemisinin and their derivatives have been used as antimalarial agents, but the emergence of a multi drug resistant (MDR) strain has diminished the therapeutic effect of these drugs.[4] Therefore, there is an urgent need to discover new, highly effective antimalarial drug candidates with new mechanisms of action to overcome the problem of the rapid emergence of drug resistance and to achieve long-term clinical efficacy.[5]

Over the past few years, triterpenoids from higher plants have shown a wide range of biological activities, such as antitumor,[6] antiviral,[7] anti-inflammatory,[8] and anti-HIV.[9] As part of our drug discovery programmes,[10–13] we recently reported significant antimalarial activity in a pentacyclic triterpenoid glycyrrhetinic acid,[14] a major constituent of *Glycyrrhiza glabra*. This encouraged us to investigate antimalarial activity in the other pentacyclic triterpenoids. A literature search revealed that ursolic acid (UA) was another such triterpenoid, occurring as major constituent in several Indian medicinal plants. Recent reports have shown that UA and its derivatives possess significant antimalarial activity,[15,16] which prompted us to develop a validated QSAR model for the antimalarial-lead optimization of UA and its derivatives.

[a]*Medicinal Chemistry Department, CSIR-Central Institute of Medicinal and Aromatic Plants, Lucknow-226015, U.P., India. E-mail: skscimap@gmail.com; Fax: +91-522-2342666; Tel: +91-522-2718581*

[b]*Molecular Bioprospection Department, CSIR-Central Institute of Medicinal and Aromatic Plants, Lucknow-226015, U.P., India*

[c]*Metabolic & Structural Biology Department, CSIR-Central Institute of Medicinal and Aromatic Plants, Lucknow-226015, U.P., India*

[d]*Academy of Scientific and Innovative Research (AcSIR), Anusandhan Bhawan, New Delhi 110 001, India*

† Electronic supplementary information (ESI) available. See DOI: 10.1039/c4ra13709d

‡ Part of Ph. D. thesis work.

§ Both authors are equally contributed.

2. Results

2.1 QSAR studies

To predict the antiplasmodial activity, a QSAR model was developed using a forward stepwise MLR approach. After much iteration, four chemical descriptors: the heat of formation (kcal mole^{-1}), lambda max UV-Visible (nm), log *P* and the shape index (basic kappa, order 2) were found to strongly correlate with the biological activity and were subsequently used in the QSAR model building (eqn (1)).

$$\begin{aligned}\text{Predicted log } IC_{50}\ (\mu g\ mL^{-1}) = {} & -0.00966819 \times \text{heat of formation (kcal mole}^{-1}) \\ & - 0.00200108 \times \text{lambda max UV-Visible (nm)} \\ & + 0.245022 \times \log P \\ & - 0.324606 \times \text{shape index (basic kappa, order 2)} \\ & - 1.05926 \end{aligned} \quad (1)$$

The derived QSAR model showed an excellent correlation between a set of model descriptors and biological activity, which is evident from the high r^2 (0.974803) and q^2 (0.965426) (Fig. 1).

Further, the Y-randomization test (average r^2 is less than 20) apparently showed that the model is robust and that the correlation is real (SI-1, Table S1†).

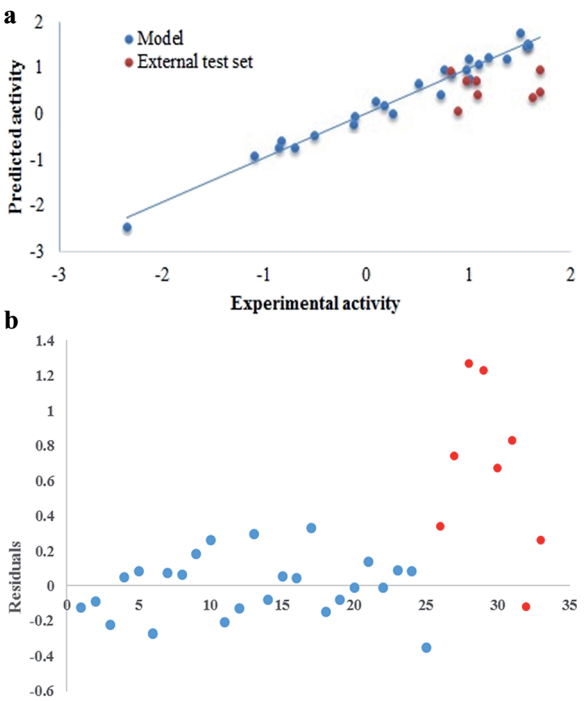

Fig. 1 (a) Scatter plot of the experimental and predicted log IC_{50} values for 25 training set compounds (blue) and the external test (UA-13, UA-17, UA-18, UA-21, UA-22, UA-14, UA-15, and UA-16) set compounds (red) showing a linear relationship. (b) Residual plot of the experimental and predicted activity (blue: training set; red: test set).

2.2 Virtual screening of the ursolic acid derivatives for antiplasmodial activity

It has been reported that the derivatization at C-3 and C-28 in triterpenoids enhances their antiplasmodial activity.[16] Therefore, with this in mind, twenty-two different types of ursolic acid virtual derivatives (termed UA-1 to UA-22, Fig. 2) were prepared and screened through the developed QSAR model against *P. falciparum* and the results are summarized in Table 1.

Out of the twenty-two derivatives, eight derivatives showed a higher predicted antiplasmodial activity (0.07–0.96 μg mL^{-1}) than the parent compound UA (1.04 μg mL^{-1}), while the rest of the derivatives showed a lower activity than the UA (1.31–1.53 μg mL^{-1}). This prompted us to carry out the semi-synthesis of these eight UA derivatives for the validation of our QSAR model.

2.3 Isolation of UA and the semi-synthesis of the UA derivatives

The isolation of UA was carried out from the leaves of *E. tereticornis* and characterized on the basis of its ^{1}H and ^{13}C NMR spectroscopic data, as reported in our earlier publication.[10] Furthermore, eight virtually-active derivatives of UA were semi-synthesized, purified and characterized according to the procedure reported in our earlier publications.[10,11]

2.4 *In vitro* antiplasmodial activity evaluation of the semi-synthetic derivatives of UA

The inhibition of the parasite growth by ursolic acid and its semi-synthetic derivatives was determined using a pLDH assay at different concentrations, and the results are presented in Table 2. Out of the eight semi-synthetic derivatives evaluated, five derivatives: UA-13, UA-17, UA-18, UA-21 and UA-22 exhibited an IC_{50} between 10.5 to 21.6 μM, *i.e.* better than the parent compound UA (IC_{50} 26 ± 0.70 μM), while three derivatives: UA-14, UA-15, and UA-16 showed lower antiplasmodial activity (IC_{50} between 73.1 to 83.2 μM) than the UA. The best antiplasmodial activity was exhibited by the derivatives UA-18 and UA-21 with IC_{50} of 12.7 ± 0.51 μM and 10.5 ± 0.49 μM, respectively. The IC_{50} for CQ and artemisinin were 0.021 ± 0.002 μM and 0.007 ± 0.004 μM, respectively.

2.5 Structure activity relationship

A total of eight virtual derivatives of UA (UA13 to UA-18, UA-21 and UA-22) were semi-synthesised and their structure activity relationship (SAR) against *P. falciparum* was derived. The UA

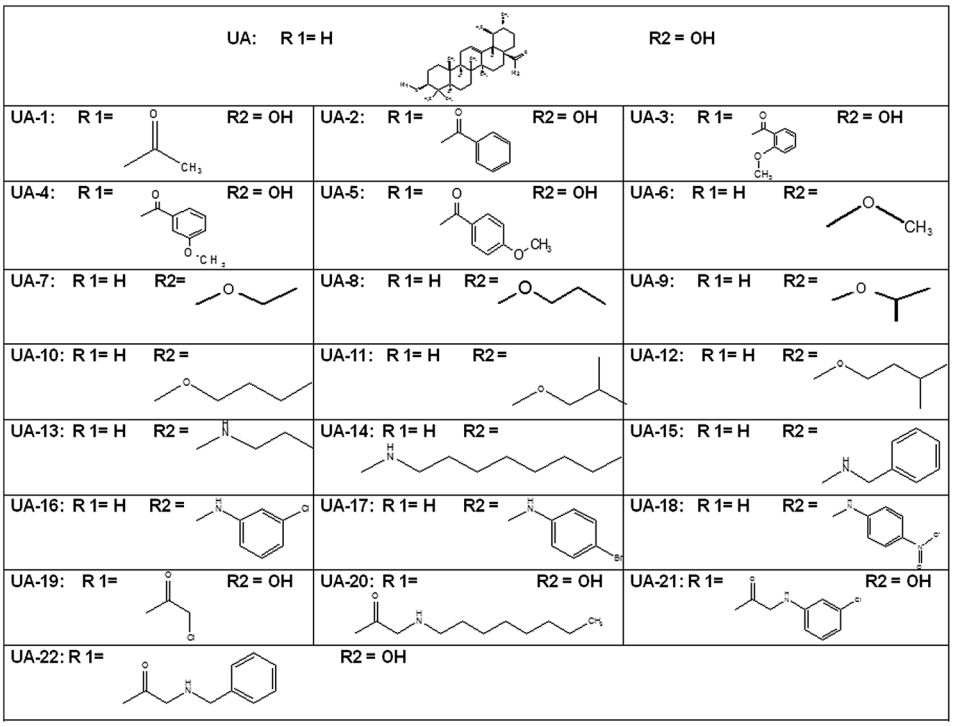

Fig. 2 Structures of the predicted virtual UA derivatives.

Table 1 Predicted antiplasmodial activities of UA and its virtual derivatives (UA-1 to UA-22) against the *P. falciparum* NF-54 strain

S. no.	Compound	Predicted activity (log μg mL^{-1})
1	UA	1.04
2	UA-1	1.449
3	UA-2	1.318
4	UA-3	1.537
5	UA-4	1.474
6	UA-5	1.441
7	UA-6	1.317
8	UA-7	1.371
9	UA-8	1.443
10	UA-9	1.434
11	UA-10	1.482
12	UA-11	1.501
13	UA-12	1.538
14	UA-13	0.73
15	UA-14	0.96
16	UA-15	0.36
17	UA-16	0.47
18	UA-17	0.42
19	UA-18	0.07
20	UA-19	1.33
21	UA-20	1.33
22	UA-21	0.94
23	UA-22	0.72
24	CQ	−2.45

derivatives UA-13 to UA-18 were prepared by modification of the C-28 carboxylic acid group, while the derivatives UA-21 and UA-22 were prepared by modification of the C-3 hydroxyl group of UA. The antiplasmodial activity results of these derivatives shown in Table 2 clearly demonstrates that the conversion of UA into its amide derivative UA-13 slightly increased the activity, but a further increase in the side chain carbons from three to eight (*i.e.* in UA-13 to UA-14) drastically reduced the activity. Similarly, the unsubstituted aryl amide derivative, UA-15, also showed a drastic reduction in activity. Furthermore, electronegative substitution at the meta position in the aryl amide derivative, UA-16, again reduced the activity. However, when the electronegative (Br) group was placed at the *para* position in aryl amide, UA-17, the activity drastically increased by fourfold to that of UA-15 and UA-16. Similarly, when a more electronegative group (NO_2) was placed at the *para* position in aryl amide, *i.e.* in UA-18, the activity increased by sixfold to that of UA-15 and UA-16 and twofold to that of the starting material UA. Among the C-3 hydroxyl derivatives, *i.e.* UA-21 and UA-22, the chloroaniline derivative UA-21 was more active than the benzyl amine derivative UA-22. From the above results, it may be concluded that UA-18 and UA-21 possess potential activity against *P. falciparum* strain (NF-54).

2.6 Effect of the UA derivatives on the intra-erythrocytic cycle of *P. falciparum*

It was found that UA derivatives (UA-18 and UA-21) arrested the progress of *P. falciparum* erythrocytic cycle. To study the effect on the maturation of the parasite stages, synchronized culture at ring stage (2.5% parasitaemia) were treated at IC_{50} and 4× IC_{50} concentrations for 60 h. Culture treated with UA-21 at IC_{50} concentration, arrested the growth of young rings but at the same time some rings got developed into trophozoites, suggested reduction in the parasitaemia in comparison to the untreated culture. At 4× IC_{50}, a large number of rings got

Table 2 Predicted and experimental antiplasmodial log IC_{50} values of UA and its derivatives

S. no.	Compound Name	Antiplasmodial activity (Clone-NF54) IC_{50} (μm)	Experimental log IC_{50}	Predicted log IC_{50}
1	UA	26 ± 0.70	1.07	1.04
2	UA-13	21.6 ± 0.79	1.07	0.73
3	UA-14	82.1 ± 0.56	1.70	0.96
4	UA-15	73.1 ± 0.60	1.63	0.36
5	UA-16	83.2 ± 0.88	1.70	0.47
6	UA-17	19.0 ± 0.44	1.09	0.42
7	UA-18	12.7 ± 0.51	0.90	0.07
8	UA-21	10.5 ± 0.49	0.82	0.94
9	UA-22	16.0 ± 0.40	0.98	0.72
10	CQ	0.021 ± 0.002	−2.34	−2.45
11	ART	0.007 ± 0.004		

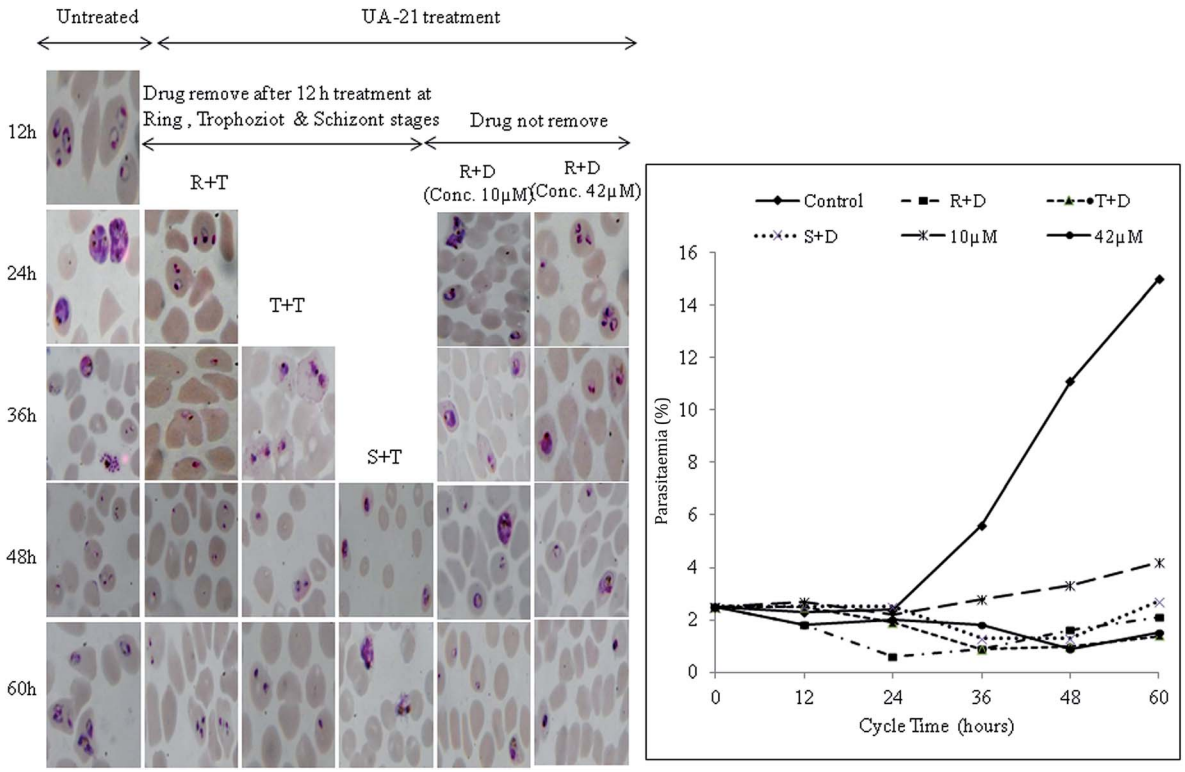

Fig. 3 Blood stage specific study of UA-21. (A) Morphological changes observed after 12 h interval up to 60 h. R + G = ring stage treated with glabridin; T + G = trophozoite stage treated with glabridin; S + G = schizont stage treated with glabridin. (B) Percent increase in the parasitaemia up to 60 h of treatment.

accumulated after 12 h treatment and no trophozoites were observed. After 24 h, the appearance of pycnotic forms and a drastic decrease in parasitaemia indicated that this dose has tendency to inhibit parasite growth completely and the inhibition were maximum at the late ring and early trophozoites stage. Further, to study whether these effects were reversible or not, 100 μM concentration was used to treated culture at ring, trophozoites and schizonts stages. After incubation, compound was removed and the parasitaemia was examined after 12 hours. The results showed that after treatment, parasitaemia was not increased in comparison to control, hence the growth of the parasite was arrested in the presence of compound and all the cultures were unable to infect the new erythrocytes after 48 h. Specific treatments at ring and trophozoites stage behaved in the same way and displayed no recovery after 12 h treatment. The treated rings were not growing normally and they could not recover after removal of the drug pressure. The appearances of ring like dots after 24 h were either the dead cells or the pycnotic form. Similarly, treated trophozoites were not able to develop in schizonts and the growth of trophozoite was arrested immediately after treatment. The parasite was not recovered after drug removal and only pycnotic forms were visible up to 60 h. The UA-21 showed similar behavior on schizonts too. After the drug removal, parasite arrest at schizonts stage was up to 48 h, but at 60 h some new rings were observed, indicating a fraction of parasite survived and developed in to new rings (Fig. 3).

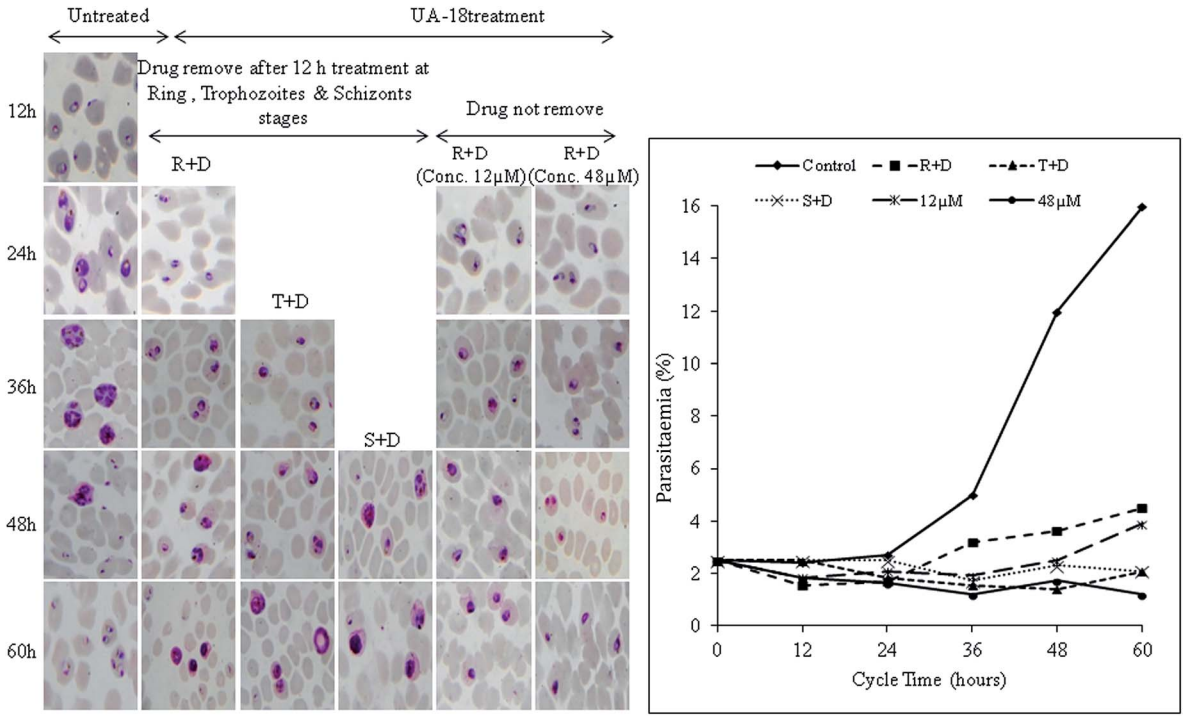

Fig. 4 Blood stage specific study of UA-18. (A) Morphological changes observed after 12 h interval up to 60 h. R + G = ring stage treated with glabridin; T + G = trophozoite stage treated with glabridin; S + G = schizont stage treated with glabridin. (B) Percent increase in the parasitaemia up to 60 h of treatment.

Culture treated with UA-18 at IC_{50} and 4× IC_{50} concentrations arrested the growth of parasite at trophozoite stage. However, the effect was most drastic at 4× IC_{50} indicated by the sharp decrease in parasitaemia as compare to IC_{50} concentration. After 24 h, the growth of parasite was arrested at trophozoite stage that was observed up to 60 h. Further, in drug reversible experiment, culture treated at ring stage showed less inhibition as compare to trophozoite stage treated culture. The growth of rings was recovered after drug removal and able to develop in trophozoite at 36 h; however parasitaemia decreased in contrast to the control (Fig. 4). Parasite treated at trophozoite stage did not recover the growth up to 60 h. At schizont stage, the parasite growth was also arrested but some new rings were observed at 60 h, indicating that a small fraction of parasite population got survived.

2.7 Binding affinity study through docking against the antimalarial target hemozoin

The plasmodium parasite can digest hemoglobin to meet its nutritional requirements and releases toxic heam (Fe^{2+}-protoporphyrin IX: Fe^{2+}-PPIX) as a byproduct. Further, heam is converted to the less toxic hematin (Fe^{3+}-PPIX), which then forms a virtually inert and harmless malaria pigment, hemozoin. Quinoline drugs are supposed to be adsorbed at the corrugated {001} face of hemozoin; thereby preventing the further deposition of heam, resulting in an accumulation of toxic-free heam and ultimately in the death of the parasite.[17] However, β-hematin is chemically, crystallographically and spectroscopically identical to hemozoin; its crystal structure was elucidated by Pagola *et al.* (2000). In the present study, the structure of the hemozoin was modelled from the unit cell of β-hematin. The prepared structure closely mimics its natural counterpart, and individual hematin units make interlocking hydrogen-bonds (O36–H37) with nearby units. The molecular docking was done by Autodock 4.2 and chloroquine was taken as the positive control. The docking results are promising and give insightful information about the binding mechanism of chloroquine and the ursolic acid derivatives. The quinoline moiety of chloroquine docked in the grooves of hemozoin (corrugated {001} face) with a high binding energy, *i.e.* −10.71 kcal mol^{-1}. This docking result confirms the proposed model of quinoline drugs binding at hemozoin's corrugated {001} face.[17] [Fig. 5a and b].

2.8 FPIX biomeneralization inhibition activity

In order to explore the mode of action of most active (IC_{50} < 20 μM) semi-synthetic derivatives of UA, their ability to inhibit β-hematin formation was studied (Table 3). A dose-dependent inhibition of β-hematin formation was studied with different concentrations of UA and its derivatives, UA-18 and UA-21. In comparison to CQ (90.8%), compound UA-21 (93.0 ± 0.11%) showed a better inhibition of β-hematin formation; however, the calculated IC_{50} for UA-21 (0.193 mM) was slightly higher than for the CQ (0.176 mM).

The docking results of UA, its two derivatives (UA-18 and UA-21) and the control CQ are presented in Table 3. The results showed that the UA-derivatives exhibited a good tendency to inhibit hemozoin. The derivative, UA-21 showed a 93% inhibition of hemozoin, which is slightly higher than that of CQ

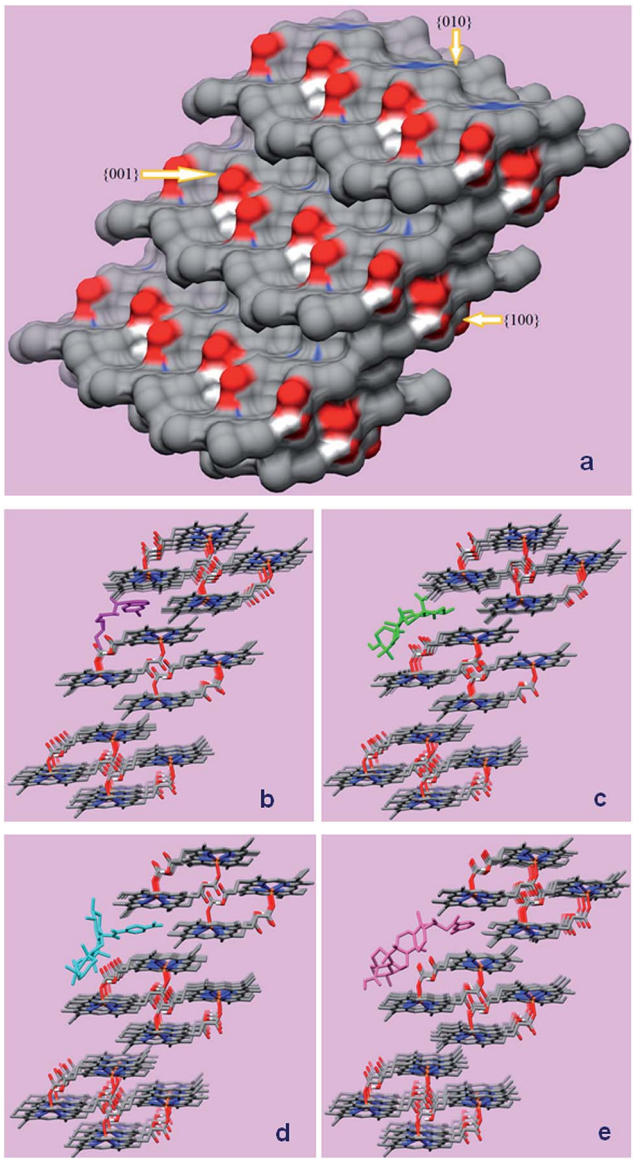

Fig. 5 (a) Hemozoin structure and docking poses; (a) surface view of modelled hemozoin showing the {100}, {010} and {001} faces. (b) Molecular structure of hemozoin corrugated face {001} docked with (a) chloroquine (CQ) (magenta), (b) ursolic acid (green), not accommodated inside the groove thus hanging outside, (c) compound UA-18 (cyan) occupying the crevice similar to CQ, and (d) compound UA-21 (pink) occupying the crevice similar to CQ.

(90%); whereas, the calculated IC_{50} of UA-21 was 193 μM, compared to CQ, which was 176 μM. This showed that UA-21 docked quite effectively to the target site.

2.9 Assessment through ADMET parameters

Recently, *in silico* ADMET analysis has become an effective approach to minimize the later stage failure of the lead candidate in the drug development process. The ADMET analysis of UA, its derivatives and CQ was performed using DS 3.5. Besides a significant antiplasmodial activity, UA and its derivatives (UA-18 & UA-21) displayed many pros and cons in term of the ADMET parameters (Table 4, Fig. 6). Unlike CQ, UA and its derivatives did not show CYP2D6 inhibition and hepatotoxicity, thus qualifying two important ADMET parameters. However, the aqueous solubility of UA and its derivatives was very low due to their highly lipophilic character, and may also be a strong point behind their poor human intestinal absorption. Notably, ursolic acid and its derivatives can be classified as non-mutagenic after TOPKAT_Ames_Prediction (DS 3.5, Accelrys, USA). Therefore, UA and its derivatives (UA-18 and UA-21) may serve as good antiplasmodial drugs under *in vivo* conditions, but need further optimization to meet good aqueous solubility and intestinal absorption levels.

2.10 Cytotoxicity against Vero cell lines

UA and its two active semi-synthetic derivatives, UA-18 and UA-21were evaluated for *in vitro* cytotoxicity against a Vero cell line using the MTT assay. UA and the derivative UA-18 did not show inhibition in the cell growth up to 100 μg mL^{-1} concentration, compared to the cell growth of control. From the Table 5, it is evident that derivative UA-21 exhibited a slender inhibition in the Vero cell growth and the calculated IC_{50} was 34.3 ± 0.33. The selectivity index (SD) was calculated for *P. falciparum* against the Vero cells. The derivatives UA-18 and UA-21 showed very high (>8) and good (3.2) selectivity indexes, respectively. The experimental SD results are presented in Table 5, together with the predicted SD results.

3. Discussion

The QSAR model was developed using an MLR approach for the screening of the virtual compounds against plasmodia, and the accuracy of the model was recorded as 96%. During the model preparation, the training data set included twenty-five known antimalarial drugs/compounds, and a total of forty-five physiochemical descriptors were used, of which four descriptors, *i.e.* the heat of formation (kcal $mole^{-1}$), lambda max UV-Visible (nm), log *P* and the shape index (basic kappa, order 2) were strongly correlated with the biological activity.

Table 3 Hemozoin and ferriprotoporphyrin IX (FPIX) biomineralization inhibition and binding energy of UA and its derivatives

S. no.	Compound name	% inhibition at 1 mM	IC_{50} (mM)	Binding energy kcal mol^{-1} (hemozoin)
1	UA	34.1 ± 1.32	1.8 ± 0.006	−6.21
2	UA-18	52.2 ± 0.3	0.605 ± 0.004	−9.50
3	UA-21	93 ± 0.11	0.193 ± 0.002	−10.38
4	CQ	90.8 ± 0.67	0.176 ± 0.001	−10.71

Table 4 *In silico* pharmacokinetic properties (ADMET) of ursolic acid and its derivatives[a]

	ADMET properties			
ADMET parameters	CQ	UA	UA-18	UA-21
ADMET_Solubility	−5.014	−7.617	−9.076	−9.302
ADMET_Solubility_Level	2	1	0	0
ADMET_Unknown_AlogP98	0	0	0	0
ADMET_BBB	0.755			
ADMET_BBB_Level	0	4	4	4
ADMET_EXT_CYP2D6	10.675	−4.36461	−12.6198	−4.71749
ADMET_EXT_CYP2D6#Prediction	TRUE	FALSE	FALSE	FALSE
ADMET_EXT_CYP2D6_Applicability#MD	8.75044	11.7927	17.4537	13.9335
ADMET_EXT_CYP2D6_Applicability#MDpvalue	0.695494	0.021236	1.36×10^{-7}	0.000347
ADMET_EXT_Hepatotoxic	−0.38675	−10.0226	−6.71596	−8.84985
ADMET_EXT_Hepatotoxic#Prediction	TRUE	FALSE	FALSE	FALSE
ADMET_EXT_Hepatotoxic_Applicability#MD	14.9992	14.8648	16.0687	17.7368
ADMET_EXT_Hepatotoxic_Applicability#MDpvalue	4.73×10^{-8}	9.39×10^{-8}	1.45×10^{-10}	6.32×10^{-15}
ADMET_Absorption_Level	0	1	3	3
ADMET_EXT_PPB	−1.84539	1.6932	−0.92305	7.37548
ADMET_EXT_PPB#Prediction	TRUE	TRUE	TRUE	TRUE
ADMET_EXT_PPBApplicability#MD	14.1972	13.8596	17.7947	18.4081
ADMET_EXT_PPBApplicability#MDpvalue	0.066835	0.137484	1.84×10^{-8}	4.33×10^{-10}
ADMET_AlogP98	4.345	6.492	7.921	8.861
ADMET_PSA_2D	27.423	58.931	99.165	77.157
TOPKAT_Ames_Prediction	Mutagen	Non-mutagen	Non-mutagen	Non-mutagen
TOPKAT_Ames_Probability	0.970111	0.000728	0.004483	0.000187
TOPKAT_Ames_Enrichment	1.73739	0.001304	0.008028	0.000335
TOPKAT_Ames_Score	10.5969	−31.7048	−27.121	−34.824

[a] Note: ADMET_Solubility_Level: 0 = extremely low, 1 = very low, 2 = low; ADMET_BBB_Level: 0 = very high, 1 = high, 2 = medium, 3 = low, 4 = undefined; ADMET_Absorption_Level: 0 = good, 1 = moderate, 2 = poor, 3 = very poor.

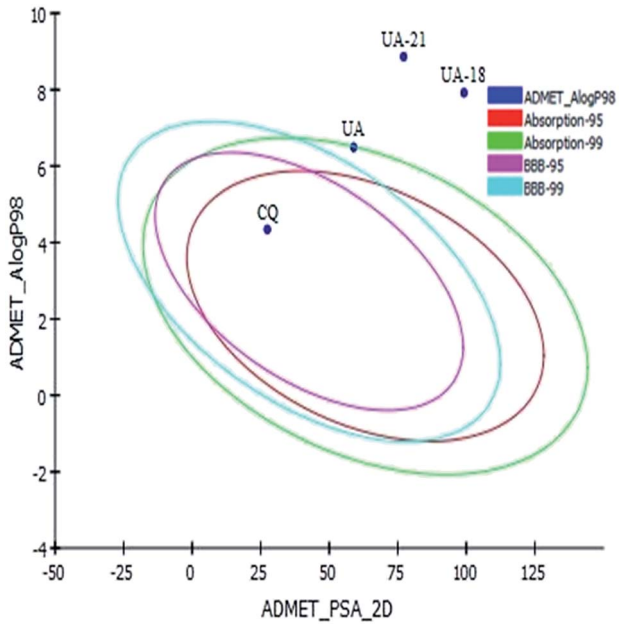

Fig. 6 ADME plot showing the compliance of UA-18 and UA-21 against bioavailability.

Furthermore, twenty-two virtual derivatives of UA were designed and screened through the developed QSAR model against anti-plasmodial activity. The predicted IC_{50} of all the derivatives was in between 0.07 and 1.5 μg mL^{-1}. Careful analysis of the results showed that out of the twenty-two, eight derivatives were significantly active and their IC_{50} values were less than the parent compound, UA (−0.07 to 0.965 μg mL^{-1}). This prompted the preparation of these virtually active derivatives in the wet laboratory.

Table 5 Cytotoxicity of UA and its derivatives

S. no.	Compound name	Cytotoxicity (Vero cell lines) IC_{50} (μm)	SD (exp.)	SD (pred.)
1	UA	>100	ND	0.02
7	UA-18	>100	>8	0.41
8	UA-21	34.3 ± 0.33	3.2	0.06
10	CQ	ND	ND	0.06

For this purpose UA was first isolated from the leaves of *E. tereticornis* and then characterized on the basis of its NMR spectroscopic data. Thereafter, the isolated UA was semi-synthetically converted into eight derivatives and these were evaluated for their anti-plasmodial potential against *P. falciparum* through a pLDH assay. Among all, the derivatives UA-18 and UA-21 showed the best activity with IC_{50} 12.7 ± 0.51 μm and 10.5 ± 0.49 μm, respectively. Further, the effects of these two derivatives were studied on the erythrocytic cycle of the parasite, and it was observed that UA-21 arrested the growth at the ring stage. In the drug reversible experiment, UA-21 inhibited growth at the ring and trophozoite stages; however,

when treated at the schizont stage, a few new rings were observed after 60 h. In the case of UA-18, parasite growth was arrested at the trophozoite stage. However, growth of the parasite was observed when treated at the ring and schizont stages.

Furthermore, the above findings were validated with the help of an *in silico* molecular docking technique. The docking of UA-18 and UA-21 was observed in the hemozoin target, and CQ was used as the positive control. The docking results show that for most of the CQ (quinoline heterocyclic aromatic ring) sandwiched deeply in the crevice with parallel orientation in respect to the porphyrin plane, cofacial pi–pi interaction seems to be the prime stabilizing force.[18] With respect to UA, compound UA-18 and UA-21 showed the highest binding energies, but they were slightly lower than CQ (Table 3). Like CQ, the side chain benzene ring of compounds UA-18 and UA-21 occupy the groove, and thus might favour cofacial pi–pi interactions and result in stable complex formation. UA, however, does not possess any such side chain, resulting in a lower binding energy. Thus, compounds which have a chemical moiety favouring pi–pi interactions within the groves of hemozoin may be preferred inhibitors against hemozoin.

Furthermore, the hemozoin inhibition was validated through a FPIX biomeneralization inhibition assay. During this assay, it was recorded that the UA-derivatives have the ability to inhibit the formation of β-hematin, which is responsible for parasitic growth. Furthermore, careful observation revealed that in comparison to UA and CQ, the derivative UA-21 had a somewhere good tendency to inhibit hemozoin formation, which is well presented in Table 3. Thus, the UA-derivatives UA-18 and UA-21 strongly correlated with their respective antiplasmodial activity, and it may be correlated that the antiplasmodial activity of these derivatives was due to the inhibition of the β-hematin formation process of *P. falciparum*.

Finally, both the UA-derivatives were *in silico* screened through ADME/T analysis and the results are presented in Table 4. Unlike CQ, UA and its derivatives did not show CYP2D6 inhibition nor hepatotoxicity, thus qualifying two important ADMET parameters. However, the aqueous solubility of UA and its derivatives was very low, due to their highly lipophilic character, which may also be a strong point behind their poor human intestinal absorption. Notably, ursolic acid and its derivatives were predicted as being non-mutagenic after TOPKAT_Ames_Prediction. Therefore, UA and its derivatives (UA-18 and UA-21) may serve as good antiplasmodial drugs under *in vivo* conditions, but need further optimization to meet good aqueous solubility and intestinal absorption levels.

4. Method and methodology

4.1 QSAR modelling

For the prediction of antiplasmodial activity in the UA derivatives, a multiple linear regression (MLR) QSAR model was developed. For this purpose, a training set of twenty-five known antimalarial drugs/compounds was prepared and their respective experimental antimalarial activities were converted into log values (SI-2, Table S2†).[15,16,19–29] The ChemBioDraw-Ultra-v12.0 software (http://www.cambridgesoft.com/) was used for sketching, geometry cleaning, energy minimization and geometry optimization of the small molecules. Energy was minimized until the root mean square (RMS) gradient value became less than 0.100 kcal mol^{-1} $Å^{-1}$ using the molecular mechanics-2 (MM2) method. The molecules were then subjected to MM2 dynamics run for 10 000 steps at a temperature of 300 K with step and frame intervals of 2.0 and 10 fs, respectively. Various topological, physicochemical and electronic descriptors were calculated using Scigress Explorer v.7.7.0.47 (Fujitsu Ltd., Poland). Initially a total of forty-five chemical descriptors were calculated for each compound (SI-3, Table S3†). Non-informative descriptors with invalid or identical values, many zeroes and highly correlated were removed. After much iteration, four descriptors were found to be strongly correlated with biological activity, and subsequently were used in the QSAR model building. A QSAR model was developed through a forward stepwise MLR approach, in which one variable was added at a time and used to test the significance of each addition. The derived QSAR model was examined through internal and external validation methods. The statistical quality of the developed QSAR model was assessed by the coefficient of determination (r^2) and was cross-validated r^2 (q^2). In addition, a Y-randomization test was performed to ensure robustness and to avoid chance correlation (Tropsha *et al.*, 2003).[30] Thereafter, the developed QSAR model was used to predict the anti-malarial activity of the ursolic acid derivatives.

4.2 General experimental procedure

^1H and ^{13}C NMR spectra of the compounds were recorded on a Bruker 300 MHz spectrometer in deuterated chloroform. The chemical shifts are in ppm with reference (internal) to tetramethylsilane (TMS) and the *J* values are in hertz. With the DEPT pulse sequence, different types of carbons (C, CH, CH_2 & CH_3) in UA and its derivatives were determined. For all the chromatographic techniques, silica gel G or H (Merck) were used (Merck, Mumbai, India). All the required solvents and reagents were purchased from Spectrochem (Mumbai, India) and Thomas Baker Pvt. Ltd., India. Pre-coated Silica gel (60F) TLC plates 0.25 mm (Merck) was used to determine the profiles of the reaction products and their purity. The developed TLC plates were first observed at 254 nm in UV and then sprayed with Bacopa reagent [vanillin–ethanol–sulphuric acid (1 g : 95 mL : 5 mL)] and the spots were visualized after heating the TLC plate at 110 °C for 5 minutes.

4.2.1 Plant material. For the isolation of UA, the leaves of *E. tereticornis* were collected from the medicinal farm of the Central Institute of Medicinal and Aromatic Plants (CIMAP), Lucknow, Uttar Pradesh, India during the January 2008 and a voucher specimen (CIMAP no. 12470) was deposited in the herbarium section of the Botany Department of CIMAP.[10]

4.2.2 Extraction and isolation of UA. The extraction, fractionation, isolation and characterization of UA was carried out according to the procedure described in our earlier publications,[10,11] while the semi-synthesis of UA derivatives are described in Schemes 1 and 2 in the SI-4.†[10,11,31]

4.3 Chemicals and materials for the antiplasmodial assay

The RPMI-1640 medium, albumax II, fetal bovine serum and fungizone were purchased from Gibco BRL (Grand Island, NY, USA). 4-(2-hydroxyethyl)-1-piperazineethanesulfonic acid (HEPES) buffer, hypoxanthine, triton X-100, L-lactic acid, 3-acetyl pyridine adenine dinucleotide (APAD), nitro blue tetrazolium (NBT), phenazine ethosulphate (PES), antibiotic-antimycotic solution (100×), phosphate buffered saline (PBS), neutral red, chloroquine diphosphate, artemisinin, doxorubicin hydrochloride, and hemin chloride were purchased form Sigma-Aldrich (St. Louis, MO, USA).

4.3.1 Parasite culture. The *P. falciparum* (NF-54) was cultivated in human B^+ red blood cells using RPMI-1640 medium supplemented with 25 mM HEPES, 0.2% $NaHCO_3$, 370 μM hypoxanthine, 40 μg mL^{-1} gentamycin, 0.25 μg mL^{-1} fungizone, and 0.5% albumax II at 37 °C using the method described by Trager and Jensen.[32] The culture was maintained in an incubator containing 5% CO_2 at 37 °C. The culture medium was changed after every 24 h, and was routinely monitored through Geimsa staining using thin smears. The culture was synchronized by 5% D-sorbitol treatment to obtain ring-stage parasites.[33]

4.3.2 Antiplasmodial activity. The UA and its derivatives were dissolved in DMSO and further diluted with culture medium to achieve the required concentrations (final concentration <1% DMSO, which were found to be non-toxic to the parasite). Parasite growth was determined spectrophotometrically by measuring the activity of the parasite lactate dehydrogenase.[34] Briefly, a synchronous ring stage culture with 1.2% parasitaemia and 2% hematocrit was incubated in a 96-well microtitre plate in different concentrations of UA and its derivatives at 37 °C for 72 h. After incubation, the plates were subjected to three 20 minute freeze–thaw cycles to release the cell content, and then the cultures were carefully mixed and aliquots of 20 μL were taken and added to another microtitre plate containing 100 μL of Malstat reagent (0.125% Triton X-100, 130 mM L-lactic acid, 30 mM Tris buffer and 0.62 μM APAD) and 25 μL of NBT-PES (1.9 μM nitro blue tetrazolium and 0.24 μM phenazine ethosulphate) solution per well. The plate was incubated in the dark for 30 min and the absorbance was recorded at 650 nm using a micro plate reader (FLUOStar Omega, BMG Labteck). All the experiments were performed in triplicate.

4.3.3 *In vitro* stage-specific effect of UA-18 and UA-21. The effects of the active derivatives UA-18 and UA-21 on the blood stages of the parasite were studied using the method described earlier, but with some modifications.[35] To study the effect on the parasite's intra-erythrocytic cycle, ring synchronized *P. falciparum* culture at 2.5% parasitaemia was incubated at IC_{50} and 4 × IC_{50} of the test compound, with a drug-free culture used as the control. In parallel, to study the stage specificity action of the most active derivatives, UA-18 and UA-21, highly synchronized ring, trophozoites and schizonts stage cultures at the same parasitaemia were incubated with 100 μM of the derivatives for 12 h. All the cultures were started using a single synchronized culture from which aliquots were taken at 12 h (for rings), 24 h (for trophozoits) and 36 h (for schizonts) and then treated for 12 h, followed by drug removal by multiple washes. Thin blood smears were made and stained with Giemsa at 12 h intervals. The parasitaemia was measured by counting 1500 red blood cells. Parasite morphology was evaluated by the microscopic analysis of Giemsa-stained thin blood smears. The cultures were monitored for at least 72 h.

4.4 Molecular docking

In the docking experiment, hemozoin was taken as a receptor molecule, while the UA derivatives and chloroquine (standard control) were taken as the ligands. The hemozoin structure was modelled from the unit cell structure of β-hematin retrieved through the Cambridge Crystallographic Database (CCD).[36] In order to prepare the receptor molecule, polar hydrogens and Gasteiger charges were added. Molecular docking was performed using Autodock 4.2, and the receptor was treated as rigid, while the ligands were flexible with active rotatable bonds.[37] A genetic algorithm (GA) was used for the docking, and the important parameters included 100 GA run for each case, initial population size of 150, the maximum number of evaluations were 2 500 000, maximum number of generations were 27 000, maximum number of individual that automatically survived was 1, gene mutation rate was 0.02, crossover rate was 0.8, GA crossover mode was two, number of generations for picking the worst individuals were 10, and the mean and variance for the Cauchy distribution for gene mutation were 0.0 and 1.0, respectively.

4.5 Ferriprotoporphyrin IX (FP) biomineralization inhibition assay

In order to determine the mode of action of UA and its most active derivatives, their ability to inhibit β-hematin (or hemozoin) formation by the ferriprotoporphyrin IX (FP) biomineralization was studied.[38] Briefly, the assay was performed in a flat bottom 96-well plates incubated at 37 °C for 18 h, and consisted of a mixture of 50 μL drug solution of different concentrations or 50 μL solvent (Negative control), 50 μL 0.5 mg mL^{-1} hemin chloride freshly dissolved in dimethylsulphoxide (DMSO), and 100 μL of 0.5 M sodium acetate buffer (pH 4.4). After incubation, the plate was centrifuged at 550×*g* for 8 min. The supernatant was discarded by vigorously flipping the plate upside down. Then the pellet was washed twice with 200 μL DMSO and centrifuged at 550×*g* for 8 min, and the supernatant was discarded. Then the pellet was dissolved in 200 μL of 0.1 M NaOH solution, and the absorbance was measured at 405 nm using a micro plate reader (FLUOStar Omega, BMG Labteck). The results were expressed as per cent of inhibition compared to the negative control (DMSO). The positive control was chloroquine (in water). All the experiments were performed in triplicate.

4.6 Screening for ADMET properties

Because of the poor pharmacokinetic and toxicity profiles (ADMET), most of the lead candidates in the drug discovery process fail to qualify clinical trials. The acronym ADMET refers

to the absorption, distribution, metabolism, excretion and toxicity properties of a drug/molecule within an organism, and were predicted by the ADMET package of Discovery Studio 3.5 (Accelrys, USA). In this package, six mathematical models (aqueous solubility, cytochrome P450 2D6 inhibition, hepatotoxicity, blood-brain barrier penetration, human intestinal absorption, and plasma protein binding) were used to predict the ADMET characteristics of the UA derivatives, quantitatively. The TOPKAT module of DS3.5 was used for toxicity prediction.[39]

4.7 Cytotoxicity against Vero cells

The cytotoxicity of the test compounds was assessed using the MTT assay, as described by Woerdenbag *et al.*, 1993.[40] Briefly, Vero cells were cultured using an RPMI-1640 medium supplemented with 0.2% $NaHCO_3$, 1× antibiotic-antimycotic solution, and 10% fetal bovine serum at 37 °C in an atmosphere of 95% humidity and 5% CO_2. The cells were seeded in 96-well flat-bottom tissue culture plates at a density of 2×10^4 cells per well in the complete medium. Different concentrations of the test compounds were added after 24 h of seeding and incubated for 48 h. After incubation, 20 μL of MTT (5 mg mL^{-1} in PBS) solution was added to each well, gently mixed and then incubated for another 4 h. After 4 h of incubation, the culture medium was removed and 150 μL of DMSO was added to each well and mixed gently. The absorbance of the control and the treated wells were measured at 590 nm using a micro plate reader (FLUOStar Omega, BMG Labteck). All the experiments were performed in triplicate. The cytotoxicity was expressed as IC_{50s} (mean ± SEM), calculated from the dose–response curve data by a nonlinear regression analysis.

4.8 Determination of the selectivity ratio

The selectivity index (SI) was used as a parameter of clinical significance. Generally, a selectivity index >2.0 is considered to be safe. The SI was calculated from the following expression as described previously.[41]

SI = IC_{50} of the test compound against Vero cells/IC_{50} of the test compounds against *P. falciparum*.

4.9 Statistical analysis

One-way analysis of variance (ANOVA) was used to analyze the mean values obtained for the treatment and control.

5. Conclusion

The QSAR-guided semi-synthesis of UA derivatives showed that two derivatives: UA-18 and UA-21 possess significant antiplasmodial activity and also showed a high binding affinity against the parasitic target hemozoin (β-hematin unit). Furthermore, the docking results were validated with an FPIX biomineralization inhibition assay. The drug likeness pharmacokinetic (PK) and cytotoxicity of UA-18 and UA-21 (ADME/Tox) were within the acceptable limits, along with a noteworthy selectivity index. Thus, the UA derivatives may serve as good antiplasmodial drugs, but require further lead optimization with respect to activity, aqueous solubility and intestinal absorption.

6. Ethics statement

After getting informed consent, B^+ human blood was obtained from volunteers for carrying out the experimentation. The study was approved by the Institutional Bio-safety Committee and Institutional Animal Ethics Committee (IAEC) of the Central Institute of Medicinal and Aromatic Plants, Lucknow followed by the Committee for the Purpose of Control and Supervision of Experimental Animals (CPCSEA), New Delhi, Government of India (Registration no: 400/01/AB/CPCSEA).

Acknowledgements

We are thankful to Director CIMAP for his keen interest and encouragement in carrying out the present work. Financial support received from CSIR Networking project BSC-0121 and one of our candidates (KK) is gratefully acknowledged for BSC-203 project. HSC & HT are grateful to ICMR for the senior research fellowship. Authors are also gratefully acknowledging the help of Dr Prema Vasudev for providing the crystal structures of heme and hematin.

References

1 R. S. Phillips, *Clin. Microbiol. Rev.*, 2001, **14**, 208–226.
2 W.H.O. (World Malaria Report), 2012, available from, http://www.who.int/malaria/publications/world_malaria_report_2012/report/en/wmr2012_full_report.pdf, accessed: August/2013.
3 J. P. Daily, *J. Clin. Pharmacol.*, 2001, **46**, 1487–1497, DOI: 10.1177/0091270006294276.
4 J. Penna-Coutinho, W. A. Cortopassi, A. A. Oliveira, T. C. França and A. U. Krettli, *PLoS One*, 2011, **6**, e21237, DOI: 10.1371/journal.pone.0021237.
5 J. R. A. Silva, A. S. Ramos, M. Machado, D. F. Moura, Z. Neto, M. M. C. Cavalheiro, P. Figueiredo, V. E. Rosário, A. C. F. Amaral and D. Lopes, *Mem. Inst. Oswaldo Cruz*, 2011, **106**, 142–157.
6 L. Novonty, A. Vachalkaov and D. Biggs, *Neoplasma*, 2001, **48**, 241–243.
7 V. Haridas, C. Arntzen and J. U. Gutterman, *Proc. Natl. Acad. Sci. U. S. A.*, 2001, **98**, 11557–11562.
8 H. Jung, J. Nam, J. Croi, K. Lee and H. Park, *Biol. Pharm. Bull.*, 2005, **28**, 101–104.
9 T. Ikeda, K. Yokomizo, M. Okawa, R. Tsuchihashi, J. Kinjo, T. Nohara and M. Uyeda, *Biol. Pharm. Bull.*, 2005, **28**, 1779–1781.
10 K. Kalani, D. K. Yadav, F. Khan, S. K. Srivastava and N. Suri, *J. Mol. Model.*, 2012, **18**(7), 3389–3413.
11 K. Kalani, D. K. Yadav, A. Singh, F. Khan, M. M. Godbole and S. K. Srivastava, *Curr. Top. Med. Chem.*, 2014, **14**(8), 1005–1013.
12 D. K. Yadav, K. Kalani, A. K. Singh, F. Khan, S. K. Srivastava and A. B. Pant, *Curr. Med. Chem.*, 2014, **21**(9), 1160–1170.

13 D. K. Yadav, K. Kalani, F. Khan and S. K. Srivastava, *Med. Chem.*, 2013, **9**(8), 1073–1084.
14 K. Kalani, J. Agarwal, S. Alam, F. Khan, A. Pal and S. K. Srivastava, *PLoS One*, 2013, **8**(9), e74761, DOI: 10.1371/journal.pone.0074761.
15 A. M. Innocente, G. N. Silva, L. N. Cruz, M. S. Moraes, M. Nakabashi, P. Sonnet, G. Gosmann, C. R. Garcia and S. C. Gnoatto, *Molecules*, 2012, **17**(10), 12003–12014.
16 S. C. B. Gnoatto, S. Susplugas, L. Dalla Vechia, T. B. Ferreira, A. Dassonville-Klimpt, K. R. Zimmer, C. Demailly, S. Da Nascimento, J. Guillon, P. Grellier, H. Verli, G. Gosmann and P. Sonnet, *Bioorg. Med. Chem.*, 2008, **16**, 771–782.
17 R. Buller, M. L. Peterson, O. Almarsson and L. Leiserowitz, *Cryst. Growth Des.*, 2002, **2**(6), 553–562.
18 S. R. Vippagunta, A. Dorn, H. Matile, A. K. Bhattacharjee, J. M. Karle, W. Y. Ellis, R. G. Ridley and J. L. Vennerstrom, *Med. Chem.*, 1999, **42**, 4630–4639.
19 J. N. Figueiredo, B. Räz and U. Séquin, *J. Nat. Prod.*, 1998, **61**(6), 718–723.
20 S. E. Lee, M. R. Kim, J. H. Kim, G. R. Takeoka, T. W. Kim and B. S. Park, *Phytomedicine*, 2008, **15**(6–7), 533–535.
21 D. A. Thiem, A. T. Sneden, S. I. Khan and B. L. Tekwani, *J. Nat. Prod.*, 2005, **68**(2), 251–254.
22 C. Ma, H. J. Zhang, G. T. Tan, N. V. Hung, N. M. Cuong, D. D. Soejarto and H. H. Fong, *J. Nat. Prod.*, 2006, **69**(3), 346–350.
23 C. Van Baren, I. Anao, P. Leo Di Lira, S. Debenedetti, P. Houghton, S. Croft and V. Martino, *Z. Naturforsch., C: J. Biosci.*, 2006, **61**(3–4), 189–192.
24 D. B. Domínguez-Carmona, F. Escalante-Erosa, K. García-Sosa, G. Ruiz-Pinell, D. Gutierrez-Yapu, M. J. Chan-Bacab, A. Gimenez-Turba and L. M. Penã-Rodríguez, *Phytomedicine*, 2010, **17**, 379–382.
25 J. Bickii, N. Njifutie, J. A. Foyere, L. K. Basco and P. Ringwald, *J. Ethnopharmacol.*, 2000, **69**(1), 27–33.
26 S. Omar, K. Godard, A. Ingham, H. Hussain, V. Wongpanich, J. Pezzuto, T. Durst, C. Eklu, M. Gbeassor, P. Sanchez-Vindas, L. Poveda, B. J. R. Philogene and J. T. Arnason, *Ann. Appl. Biol.*, 2003, **143**, 135–141.
27 N. Saewan, J. D. Sutherland and K. Chantrapromma, *Phytochemistry*, 2006, **67**(20), 2288–2293.
28 A. A. da Silva Filho, D. O. Resende, M. J. Fukui, F. F. Santos, P. M. Pauletti, W. R. Cunha, M. L. Silva, L. E. Gregório, J. K. Bastos and N. P. Nanayakkara, *Fitoterapia*, 2009, **80**(8), 478–482.
29 G. N. da Silva, N. R. Maria, D. C. Schuck, L. N. Cruz, M. S. de Moraes, M. Nakabashi, C. Graebin, G. Gosmann, C. R. Garcia and S. C. Gnoatto, *Malar. J.*, 2013, **12**, 89.
30 A. Tropsha, P. Gramatica and V. K. Gombar, *The Importance of Being Earnest: Validation is the Absolute Essential for Successful Application and Interpretation of QSPR Models*, QSAR & Combinatorial Science, April 2003, vol. 22, issue 1, pp. 69–77.
31 R. Csuk, S. Schwarz, R. Kluge and D. Strohl, *Eur. J. Med. Chem.*, 2010, **45**, 5718–5723.
32 W. Trager and J. B. Jensen, *Science*, 1976, **193**, 673–675.
33 C. Lambros and J. P. Vanderberg, *J. Parasitol.*, 1979, **65**, 418–420.
34 M. T. Makler and D. J. Hinrichs, *Am. J. Trop. Med. Hyg.*, 1993, **48**, 205–210.
35 H. S. Cheema, O. Prakash, A. Pal, F. Khan, D. U. Bawankule and M. P. Darokar, *Parasitol. Int.*, 2014, **63**, 349–358.
36 S. Pagola, P. W. Stephens, D. S. Bohle, A. D. Kosar and S. K. Madsen, *Nature*, 2000, **404**(6775), 307–310.
37 G. M. Morris, R. Huey, W. Lindstrom, M. F. Sanner, R. K. Belew, D. S. Goodsell and A. J. Olson, *J. Comput. Chem.*, 2009, **30**(16), 2785–2791.
38 E. Deharo, R. N. Garcia, P. Oporto, A. Gimenez, M. Sauvain, V. Jullian and H. Ginsburg, *Exp. Parasitol.*, 2002, **100**, 252–256.
39 Accelrys Software Inc., *Discovery Studio Modeling Environment, Release 3.5*, Accelrys Software Inc., San Diego, 2013.
40 H. J. Woerdenbag, T. A. Moskal, N. Pras, T. M. Malingre, E. S. EI-Feraly, H. H. Kampinga and A. W. T. Konings, *J. Nat. Prod.*, 1993, **56**, 849–856.
41 B. S. Sisodia, A. S. Negi, M. P. Darokar, U. N. Dwivedi and S. P. S. Khanuja, *Chem. Biol. Drug Des.*, 2012, **79**, 610–615.